

Electrostatic interactions of charged bodies from the weak to the strong coupling regime

Marius M. Hatlo and Leo Lue*
School of Chemical Engineering and Analytical Science
The University of Manchester
PO Box 88
Sackville Street
Manchester M60 1QD
United Kingdom
 (Dated: February 2, 2022)

A simple field theory approach is developed to model the properties of charged, dielectric bodies and their associated counterions. This predictive theory is able to accurately describe the properties of systems (as compared to computer simulation data) from the weak coupling limit, where the Poisson-Boltzmann theory works well, through to the strong coupling limit. In particular, it is able to quantitatively describe the attraction between like-charged plates and the influence of image charge interactions.

Electrostatic interactions play a major role in determining the structure and thermodynamics of many colloidal and biological solutions, which typically contain charged macromolecular structures with low dielectric interiors, such as DNA, charged micelles, or membranes. These charged structures are always surrounded by neutralizing counterions, and, in many cases, the properties of the system can be mainly attributed to properties of the counterions [1].

When the electrostatic interactions are weak, their contributions to the system properties are accurately described by the Poisson-Boltzmann (PB) theory. However, as these interactions strengthen, the PB theory becomes less and less accurate. Perturbation methods, such as the loop expansion can be used to systematically improve the theory; however, the first loop correction offers only a small improvement [1, 2, 3], and higher-order corrections are increasingly complicated to evaluate.

When the electrostatic interactions are extremely strong (e.g., when the surface charge of the macromolecular structures or the valency of the counterions is high), the Poisson-Boltzmann theory can yield *qualitatively* incorrect predictions. For example, in this regime, the counterions can generate attractive forces between similarly charged objects [4]. This phenomenon cannot be explained by the PB theory, but has been observed in Monte Carlo simulations [4] and in experiments (e.g., condensation of DNA molecules [5], bundle formation of filamentous actin [6]). In this strong coupling regime, the counterions “collapse” on the neutralizing charged surfaces to form a highly interacting 2D structure that resembles a confined one-component plasma (OCP) [7, 8, 9]. In these systems, the average distance a_{\perp} between the ions is much larger than the average distance z between the ions and the charged surface (i.e. $z \ll a_{\perp}$). Consequently, a single particle theory provides a good description of the system. This leads to the strong coupling (SC) expansion [8, 10], which has been quite successful [11, 12, 13].

However, many systems are in a regime where both the PB theory and SC expansion are inaccurate. The behavior of these systems can be rationalized in terms of a correlation hole [14] — a region of size σ around each counterion where it is unfav-

orable for other counterions to be located. At length scales greater than σ , the counterions are weakly correlated, while at shorter length scales, the counterions are strongly correlated but fairly “isolated” [10]. In the weak coupling regime, the counterions form a diffuse 3D layer, and the size of the correlation hole is approximately equal to the Bjerrum length $l_B = \beta q^2 / \epsilon$ (where q is the counterion charge), the distance at which two counterions interact with energy $k_B T$. In the SC limit, the size of the correlation hole becomes equal to the average (2D) distance between the ions $a_{\perp} = 2\mu\sqrt{2l_B/\mu}$, where $\mu = (2\pi\beta q\Sigma)^{-1}$ is the Gouy-Chapman length (where Σ is the surface charge density), the distance at which the interaction between a counterion and the charged surface equals $k_B T$.

Based on this observation, Weeks and coworkers [15] and Santangelo [16] developed approaches that split the interaction between the ions at short and long range. The long-range interaction is treated within a mean field approximation, and the short-range interactions with a more precise approach (e.g., computer simulation, liquid state theory, etc.). With an appropriate value for σ , these approaches can successfully describe Monte Carlo results for the full range of electrostatic coupling. However, the value of σ is determined empirically. Additionally, these approaches are not capable of describing systems with dielectric inhomogeneities.

In this work, we present a self-consistent theory that is in good agreement with Monte Carlo simulations at weak, intermediate, and strong coupling. The theory is similar in idea to the work of Weeks and coworkers [15] and Santangelo [16], however, the parameter σ is calculated consistently from the partition function, rather than chosen empirically or adjusted to fit data. In addition, the theory accurately describes the presence of dielectric bodies, even in the SC limit, which has not been demonstrated by any previous theory. For the two plate system in the presence of image charges, the system undergoes a transition from a two peak density profile to a one peak density profile.

We limit our attention to systems composed of a fixed charge distribution $\Sigma(\mathbf{r})$ that is surrounded by a neutralizing cloud of counterions, which are point charges of magnitude

q immersed in a medium with dielectric constant ϵ and possibly in the presence of dielectric inhomogeneities. The total electrostatic energy H of the system is given by

$$H = \frac{1}{2} \int d\mathbf{r} d\mathbf{r}' Q(\mathbf{r}) G_0(\mathbf{r}, \mathbf{r}') Q(\mathbf{r}') - \sum_k \frac{q^2}{2} G_{\text{free}}(\mathbf{r}_k, \mathbf{r}_k) \quad (1)$$

where $Q(\mathbf{r}) = q \sum_k \delta^d(\mathbf{r} - \mathbf{r}_k) + \Sigma(\mathbf{r})$ is the total charge density, \mathbf{r}_k is the position of counterion k , G_0 is the Green's function of the associated electrostatics problem (including the effects of dielectric objects), and G_{free} is the Green's function in the absence of dielectric inhomogeneities.

To separate short and long wavelength phenomena, we split [15, 16, 17] the Green's function G_0 into a short wavelength G_s and a long wavelength G_l component

$$G_0(\mathbf{r}, \mathbf{r}') = G_s(\mathbf{r}, \mathbf{r}') + G_l(\mathbf{r}, \mathbf{r}') \quad (2)$$

where $G_s = (1 - \mathcal{P})G_0$, and $G_l = \mathcal{P}G_0$. The operator \mathcal{P} filters out the short wavelengths; its specific form is arbitrary, and in this work we use $\mathcal{P} = [1 - \sigma^2 \nabla^2 + \sigma^4 \nabla^4]^{-1}$, where σ is the length scale which divides the long from the short wavelength phenomena.

Equation (1) can be written as:

$$H = \frac{1}{2} \int d\mathbf{r} d\mathbf{r}' Q(\mathbf{r}) G_l(\mathbf{r}, \mathbf{r}') Q(\mathbf{r}') + E^{\text{se}} + \frac{q^2}{2} \sum_{jk} G_s(\mathbf{r}_j, \mathbf{r}_k) + \sum_k \left[u(\mathbf{r}_k) - \frac{q^2}{2} G_s(\mathbf{r}_k, \mathbf{r}_k) - \frac{q^2}{2} \mathcal{P} \delta G_0(\mathbf{r}_k, \mathbf{r}_k) \right] \quad (3)$$

where $\delta G_0 = G_0 - G_{\text{free}}$, $u(\mathbf{r})$ is a one-particle interaction potential given by

$$u(\mathbf{r}) = q \int d\mathbf{r}' G_s(\mathbf{r}, \mathbf{r}') \Sigma(\mathbf{r}') + \frac{q^2}{2} \delta G_0(\mathbf{r}, \mathbf{r}) - \frac{q^2}{2} \mathcal{P} G_{\text{free}}(\mathbf{r}, \mathbf{r}), \quad (4)$$

and E^{se} is the self energy of the fixed charges, defined as

$$E^{\text{se}} = \frac{1}{2} \int d\mathbf{r} d\mathbf{r}' \Sigma(\mathbf{r}) G_s(\mathbf{r}, \mathbf{r}') \Sigma(\mathbf{r}'). \quad (5)$$

By performing a Hubbard-Stratonovich transformation [18, 19] twice on the grand partition function of the system, two fields are introduced: ψ_l , which is associated with G_l and represents interactions at length scales greater than σ , and ψ_s , which is associated with G_s and represent interactions at length scales less than σ . In the approximation scheme we pursue, the one-particle contribution to the partition function is treated exactly, while the interaction between the particles is

treated approximately. The field ψ_s is strongly fluctuating and coupled not only to itself, but also to the field ψ_l . To evaluate the functional integration over ψ_s , we use a cumulant expansion, truncated at first order. This leads to an approximation similar to the SC expansion of Moreira and Netz [10, 20].

Performing the functional integration over ψ_s , we get an effective field theory for the long wavelength system. The expression for the grand partition function Z_G is

$$\ln Z_G[\gamma, \Sigma] = -\beta E^{\text{se}} + \ln \left\{ \frac{1}{\mathcal{N}_l} \int \mathcal{D}\psi_l(\cdot) e^{-H_l[\psi_l]} \right\} \quad (6)$$

and H_l is the effective Hamiltonian, which is a functional of the field ψ_l given by

$$-H_l[\psi_l] \approx -\frac{1}{2\beta} \int d\mathbf{r} d\mathbf{r}' \psi_l(\mathbf{r}) G_l^{-1}(\mathbf{r}, \mathbf{r}') \psi_l(\mathbf{r}') + \int d\mathbf{r} \Lambda^{-3} e^{\gamma - q i \psi_l(\mathbf{r}) - \beta u(\mathbf{r}) + \frac{\beta q^2}{2} \delta G_l(\mathbf{r}, \mathbf{r})} - \int d\mathbf{r} \Sigma(\mathbf{r}) i \psi_l(\mathbf{r}). \quad (7)$$

The long-wavelength field ψ_l is weakly fluctuating, so a mean-field approximation is sufficient to evaluate the functional integral over ψ_l in Eq. (6):

$$\ln Z_G[\gamma, \Sigma] = +\frac{1}{2\beta} \int d\mathbf{r} d\mathbf{r}' i \bar{\psi}_l(\mathbf{r}) G_l^{-1}(\mathbf{r}, \mathbf{r}') i \bar{\psi}_l(\mathbf{r}') - \int d\mathbf{r} \Sigma(\mathbf{r}) i \bar{\psi}_l(\mathbf{r}) - \beta E^{\text{se}} + \int d\mathbf{r} \Lambda^{-3} e^{\gamma - q i \bar{\psi}_l(\mathbf{r}) - \beta u(\mathbf{r})}, \quad (8)$$

The value of the mean field $\bar{\psi}_l(\mathbf{r})$ is determined by solving the Poisson equation

$$-\frac{1}{4\pi} \nabla \cdot \epsilon(\mathbf{r}) \nabla \phi(\mathbf{r}) = \Sigma(\mathbf{r}) + q \rho(\mathbf{r}), \quad (9)$$

where the electric potential is defined as $\beta \phi = \mathcal{P}^{-1} i \bar{\psi}_l$, and the counterion density distribution $\rho(\mathbf{r})$ is given by

$$\rho(\mathbf{r}) = \Lambda^{-3} e^{\gamma - q i \bar{\psi}_l(\mathbf{r}) - \beta u(\mathbf{r})}. \quad (10)$$

Note that the density depends on the field $\bar{\psi}_l = \mathcal{P} \phi$ rather than on the electric potential ϕ , as in the PB theory. In the systems we consider, where there are only counterions, the chemical potential γ is determined by the electroneutrality constraint.

All properties of the system should be independent of the parameter σ ; however, because the theory is approximate, there will be a dependence on the value of σ . Based on this, we determine the value of σ by requiring that the grand partition function is stationary with respect to σ (i.e. $\partial \ln Z_G[\gamma] / \partial \sigma = 0$). This is similar to the optimized random phase approximation [21].

Now we apply the theory to a system of counterions confined to one side of a plate with dielectric constant ϵ' and a uniform surface charge $\Sigma(\mathbf{r}) = \delta(z) \Sigma$, where z is the distance

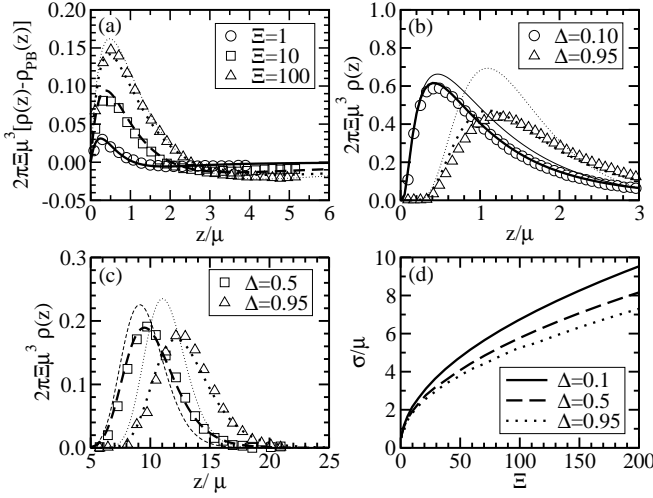


FIG. 1: (a) Counterion density profile near a single charged plate with $\Delta = 0$. Counterion density profile for (b) $\Xi = 10$ and (c) $\Xi = 1000$ near a single charged, dielectric plate. (d) Dependence of the parameter σ with the coupling parameter Ξ . The symbols are Monte Carlo simulation data [11, 22, 23], the thin lines are the predictions of the SC expansion [11, 22, 23], and the thick lines are from the present work.

from the surface of the plate. For this system, the one-body potential of the counterions (see Eq. (4)) reduces to

$$\beta u(\mathbf{r}) = -\frac{2\sigma}{\sqrt{3}\mu}(1+\Delta)e^{-\frac{\sqrt{3}z}{2\sigma}}\cos\frac{z}{2\sigma} + \frac{l_B\Delta}{4z} - \frac{l_B}{2\sqrt{3}\sigma}, \quad (11)$$

where z is the distance from the surface of the plate, and $\Delta = (\epsilon' - \epsilon)/(\epsilon' + \epsilon)$. The self energy of the surface charge (see Eq. (5)) is $\beta E^{se}/N = \frac{\sigma}{\sqrt{3}\mu}(1+\Delta)$ where N is the total number of counterions in the system. The strength of the electrostatic interactions is characterized by the parameter $\Xi \equiv l_B/\mu$.

The deviations of the counterion density profile from the predictions of the PB theory for the single plate system are plotted in Fig. 1a in the case when there is no dielectric interface (i.e. $\Delta = 0$). As the strength of the electrostatic interactions increases, the PB theory overpredicts the repulsion between the counterions and the ion cloud associated with the charged surface, and, consequently, it underestimates the adsorption of the counterions to the surface. The SC limit (given by the thin line) is only approached at fairly high values of the coupling parameter ($\Xi > 100$). The predictions of the present theory are, however, in good agreement with Monte Carlo simulation data, exhibiting the crossover of the density profile from the PB theory to the SC limit with increasing values of Ξ .

When the plate has a low dielectric interior (i.e. $\epsilon' < \epsilon$, $\Delta > 0$), repulsive image charge interactions with the plate repel the counterions from the surface, which oppose the attractive interactions with the surface charge. Consequently, the

counterions no longer collapse onto the surface, but instead peak at a distance away from the surface [24, 25, 26]. Counterion density profiles for this situation are plotted in Figs. 1b and c. When $\Delta > 0$, the SC expansion fails to accurately describe the Monte Carlo data, even well into strong coupling regime ($\Xi = 1000$). The failure of the SC theory is due to the fact that the average distance between the ions and the distance to the charged plate are the same order of magnitude. Interactions between the counterions become significant, and the physical basis for the SC is no longer fulfilled.

Our approach is able to overcome these difficulties because in addition to including the one-body interactions with the plate interactions, which occur at length scales less than σ , it also accounts for the interaction between ions at length scales greater than σ . The variation of σ with the coupling parameter Ξ is plotted for various values of Δ in Fig. 1d. For high values of the coupling parameter, the size of the correlation hole quickly approaches a constant with respect to the spacing a_\perp between the counterions. As Δ increases, the size of the correlation hole decreases, reflecting the increasing importance of the interactions between the counterions.

Now we consider systems where the counterions are confined between two uniformly charged plates, separated by a distance d . Fig. 2a shows the counterion density profile where the plates have dielectric constant $\epsilon' = \epsilon$ and are separated by a distance $d/\mu = 2$; results for the pressure are shown in Fig. 2b. At weak couplings, the force between the plates is strictly repulsive, but as Ξ increases, a region of attraction develops at intermediate plate separations. The predictions of this work are in quantitative agreement with the computer simulation data [10], while the SC limit is applicable only at extremely high values of the coupling parameters ($\Xi \sim 10^5$ for the pressure, see Ref. [10]).

Decreasing the dielectric constant of the plates ($\epsilon' < \epsilon$) leads [12, 27] to a qualitatively different counterion density profile, as shown in Fig. 3a. For sufficiently large plate separations, there is a counterion peak next to each plate. When the distance between the plates is smaller or comparable to the average distance between the ions ($a_\perp/\mu \approx \sqrt{2\Xi}$, so $d/\mu < \sqrt{2\Xi}$), the repulsive image charge interactions push the counterions into a single peak in the middle of the plates. At these separations, the distance between an ion and its image charge is comparable to the average distance between the ions. The variation of the mid-point counterion density with the coupling constant is shown in Fig. 3b. The predictions of the present work are in good agreement recent Monte Carlo simulation results for all conditions examined. The SC theory [12, 13] is only accurate when $d/\mu \ll \sqrt{2\Xi}$. The parameter σ (see Fig. 3c) increases with increasing values of Ξ and decreasing values of Δ , in a similar manner with the one plate case.

The approach developed here is applicable to general geometries (e.g., spherical or cylindrical) in the same manner as the Poisson-Boltzmann equation. The only difference will be the form of the fixed charge density $\Sigma(\mathbf{r})$. Once this is given, the one particle potential is obtained by Eq. (4) and the den-

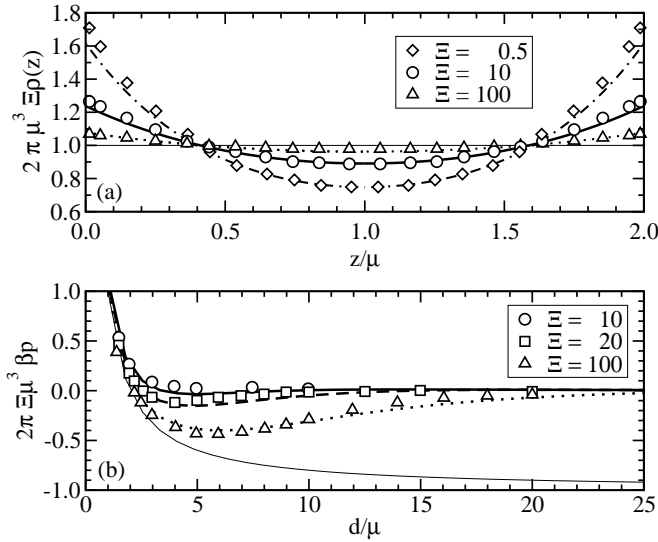


FIG. 2: (a) Density profile for counterions confined between two charged plates with $\Delta = 0$ separated by distance $d = 2\mu$. (b) Force between the plates as a function of their separation d . The symbols are simulations data [10], the thin lines are the prediction of the SC theory [10], and the thick lines are from this work.

sity by Eq. (10). The electric potential is obtained from the solution of the Poisson equation (see Eq. (9)), which can be solved by standard methods [15, 16]. This theory can also be systematically improved by either increasing the order of the cumulant expansion for the integration over ψ_s or by going beyond the mean field theory for ψ_l .

We thank Prof. C. Holm and Dr. M. Sega for providing us with unpublished simulation data for the two plate system. MM Hatlo acknowledges support from an EC Marie Curie Fellowship (MEST-CT-2004-503750).

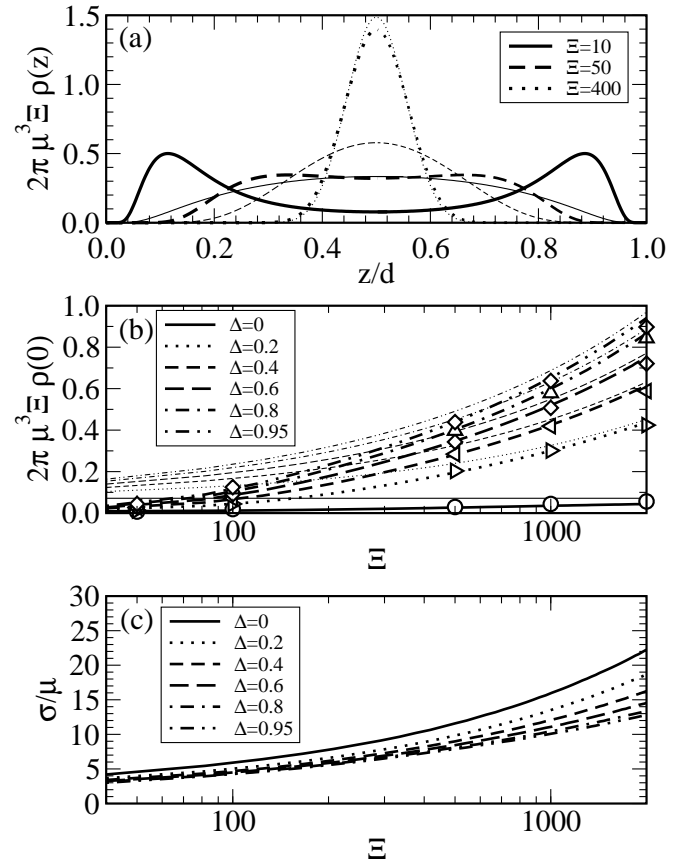


FIG. 3: (a) Density profile for counterions confined between charged plates with $\Delta = 0.98$ and $d = 10\mu$. (b) Counterion density at the mid-point between charged plates separated by distance $d = 14\mu$ and (c) the corresponding variation of the parameter σ . The symbols are Monte Carlo simulation data [13], the thin lines are the prediction of the SC theory [10, 12, 13], and the thick lines are from this work.

* Electronic address: leo.lue@manchester.ac.uk
[1] A. Naji, S. Jungblut, A. G. Moreira, and R. R. Netz, *Physica A* **352**, 131 (2005).
[2] R. Podgornik, *J. Phys. A* **23**, 275 (1990).
[3] P. Attard, D. J. Mitchell, and B. W. Ninham, *J. Chem. Phys.* **88**, 4987 (1988).
[4] L. Guldbrand, B. Jönsson, H. Wennerstrom, and P. Linse, *J. Phys. Chem.* **80**, 2221 (1984).
[5] V. A. Bloomfield, *Biopolymers* **44**, 269 (1997).
[6] J. Tang and P. A. Janmey, *J. Biol. Chem.* **271**, 8556 (1996).
[7] R. C. Gann, S. Chakravarty, and G. V. Chester, *Phys. Rev. B* **20**, 326 (1979).
[8] B. I. Shklovskii, *Phys. Rev. E* **60**, 5802 (1999).
[9] Y. Levin, *Rep. Prog. Phys.* **65**, 1577 (2002).
[10] A. G. Moreira and R. R. Netz, *Phys. Rev. Lett.* **87**, 078301 (2001).
[11] A. G. Moreira and R. R. Netz, *Europhys. Lett* **57**, 911 (2002).
[12] M. Kanduc and R. Podgornik, *Eur. Phys. J. E* **23**, 265 (2007).
[13] Y. S. Jho, M. Kanduč, A. Naji, R. Podgornik, M. W. Kim, and P. A. Pincus, *Phys. Rev. Lett.* **101**, 188101 (2008).

[14] S. Nordholm, *Chem. Phys. Lett.* **105**, 302 (1984).
[15] Y.-G. Chen and J. D. Weeks, *Proc. Nat. Acad. Sci. (USA)* **103**, 7560 (2006).
[16] C. D. Santangelo, *Phys. Rev. E* **73**, 041512 (2006).
[17] J. M. Rodgers, C. Kaur, Y.-G. Chen, and J. D. Weeks, *Phys. Rev. Lett.* **97**, 097801 (2006).
[18] J. Hubbard, *Phys. Rev. Lett.* **3**, 77 (1959).
[19] R. L. Stratonovich, *Dokl. Akad. Nauk SSSR* **115**, 1097 (1957).
[20] A. G. Moreira and R. R. Netz, *Europhys. Lett.* **52**, 705 (2000).
[21] H. C. Andersen and D. Chandler, *J. Chem. Phys.* **57**, 1918 (1972).
[22] A. G. Moreira and R. R. Netz, *Eur. Phys. J. E* **8**, 33 (2002).
[23] A. G. Moreira, Ph.D. thesis, Max-Planck-Institut für Kolloid- und Grenzflächenforschung in Golm (2001).
[24] D. Henderson, D. Gillespie, T. Nagy, and D. Boda, *Mol. Phys.* **103**, 2851 (2005).
[25] L. B. Bhuiyan, C. W. Outhwaite, D. Henderson, and M. Alawneh, *Mol. Phys.* **105**, 1395 (2007).
[26] M. M. Hatlo, R. A. Curtis, and L. Lue, *J. Chem. Phys.* **128**, 164717 (2008).
[27] M. Hatlo and L. Lue, *Soft Matter* **4**, 1 (2008).